1-1-2013

Self-similar vortex dynamics in superfluid He-4 under the Cartesian representation of the Hall-Vinen model including superfluid friction

Robert A. Van Gorder
University of Central Florida

Self-similar vortex dynamics in superfluid ^{4}He under the Cartesian representation of the Hall-Vinen model including superfluid friction

Robert A. Van Gorder

Citation: Physics of Fluids **25**, 095105 (2013); doi: 10.1063/1.4821809
View online: https://doi.org/10.1063/1.4821809
View Table of Contents: http://aip.scitation.org/toc/phf/25/9
Published by the American Institute of Physics

PHYSICS OF FLUIDS **25**, 095105 (2013)

Self-similar vortex dynamics in superfluid ^{4}He under the Cartesian representation of the Hall-Vinen model including superfluid friction

Robert A. Van Gorder[a)]
Department of Mathematics, University of Central Florida, Orlando, Florida 32816-1364, USA

(Received 17 June 2013; accepted 6 September 2013; published online 25 September 2013)

We determine conditions under which the fully nonlinear form of the local induction approximation (LIA) governing the motion of a vortex filament in superfluid ^{4}He (that is, the Hall-Vinen model) in the Cartesian frame of reference permits the existence of self-similar solutions, even in the presence of superfluid friction parameters. Writing the Cartesian Hall-Vinen LIA in potential form for the motion of a vortex filament, we find that a necessary condition for self-similarity is that the normal-fluid component vanishes (which makes sense in the low temperature limit), and we reduce the potential form of the Hall-Vinen LIA to a complex nonlinear ordinary differential equation governing the behavior of a similarity solution. In the limit where superfluid friction parameters are negligible, we provide some analytical and asymptotic results for various regimes. While such analytical results are useful for determining the qualitative behavior of the vortex filament in the limit where superfluid friction parameters vanish, numerical simulations are needed to determine the true behavior of the filaments in the case of non-zero superfluid friction parameters. While the superfluid friction parameters are small, the numerical results demonstrate that the influence of the superfluid friction parameters on the self-similar vortex structures can be strong. We classify two types of filaments from the numerical results: singular filaments (which demonstrate growing oscillations and hold kink-type solutions as a special case) and bounded filaments (whose behavior is a bounded function of x). We also comment on how to include the case where there is a non-zero normal fluid, and we find a transformation of the self-similar solutions into non-similar solutions that can account for this. [http://dx.doi.org/10.1063/1.4821809]

I. INTRODUCTION

The self-induced velocity of the vortex in the reference frame moving with the superfluid according to the local induction approximation (LIA) is given in non-dimensional form by Hall and Vinen[1,2] (see also Bekarevich and Khalatnikov[3] – this model is sometimes referred to as the HVBK, or Hall-Vinen-Bekarevich-Khalatnikov, model)

$$\mathbf{v} = \gamma\kappa\mathbf{t}\times\mathbf{n} + \alpha\mathbf{t}\times(\mathbf{U} - \gamma\kappa\mathbf{t}\times\mathbf{n}) - \alpha'\mathbf{t}\times(\mathbf{t}\times(\mathbf{U} - \gamma\kappa\mathbf{t}\times\mathbf{n})), \tag{1}$$

where $\mathbf{U}$ is the dimensionless normal fluid velocity, $\mathbf{t}$ and $\mathbf{n}$ are the unit tangent and unit normal vectors to the vortex filament, κ is the dimensionless average curvature, $\gamma = \Gamma\ln(c/\kappa a_0)$ is a dimensionless composite parameter (Γ is the dimensionless quantum of circulation, c is a scaling factor of order unity, $a_0 \approx 1.3\times10^{-8}$ cm is the effective core radius of the vortex), α and α' are dimensionless friction coefficients which are small (except near the λ-point; for reference, the λ-point is the temperature (≈ 2.17 K, at atmospheric pressure) below which normal fluid helium

a)Email: rav@knights.ucf.edu

transitions to superfluid helium[4]). Regarding reasonable values of α and α', Table 1 of Schwarz[5] shows that at temperature $T = 1$ K we have $\alpha = 0.005$ and $\alpha' = 0.003$, while at temperature $T = 1.5$ K we have $\alpha = 0.073$ and $\alpha' = 0.018$. Thus, it makes sense to consider these friction terms as small parameters. In the limit $(\alpha, \alpha') \to (0, 0)$, we recover the classical Da Rios equations for the motion of a vortex filament in a standard fluid.[6–8] In keeping both small parameters α and α', we ensure that the model accounts for superfluid friction terms. We shall refer to the model in the limit $\alpha, \alpha' \to 0$ as the standard fluid model, whereas we shall refer to the $\alpha > 0, \alpha' > 0$ case as the Hall-Vinen superfluid model.

In the present paper, we shall demonstrate that self-similar solutions exist to the vortex filament problem (1) for superfluid ^{4}He, even in the presence of superfluid friction parameters, under the Hall-Vinen model in the natural Cartesian coordinate frame (hereafter referred to as the Cartesian form of the LIA, or the extrinsic coordinate model). We shall then explore various properties of these vortex filament solutions. Previously, Lipniacki[9,10] demonstrated self-similarity for a version of the corresponding local induction equation where the dependent quantities were curvature and torsion (this is the classical intrinsic coordinate frame). In both studies, the normal fluid flow was taken to be zero, and the influence of the superfluid parameters on the curvature and torsion was studied. Thus, while self-similar solutions have been shown for the intrinsic coordinate system with curvature and torsion, self-similar solutions have not been considered for the extrinsic Cartesian form of the LIA. Such solutions for the extrinsic form of the LIA would be useful, since the extrinsic frame of reference corresponds directly to the physical geometry of the problem in Cartesian coordinates. For a mathematical treatment of similarity solutions in the curvature-torsion reference frame, see Ref. 11. The case studied therein was for the standard fluid model, corresponding to the $\alpha, \alpha' \to 0$ limit. Additionally, note that the $\alpha, \alpha' \to 0$ limit corresponds to the zero temperature limit. Svistunov explored this case in Ref. 12, and proposed a model in Cartesian coordinates.

In Sec. II, we obtain the potential form of the Hall-Vinen model and reduce it, through an appropriate similarity transformation, into a complex-valued ordinary differential equation with appropriate choice of similarity variable. To do so, we must assume that the normal fluid velocity is zero, as way done by Lipniacki[9,10] in the curvature-torsion frame. In the case of very small superfluid friction, the parameters α and α' drop out, and we may obtain some analytical results corresponding to the temperature zero limit. These results allow us to understand the qualitative features of some of the interesting solutions, and are highlighted in Sec. III. Most interesting are the small amplitude solutions (which measure small deviations of the vortex filament from its central axis of rotation) and asymptotic solutions, valid for large values of the similarity variable. In Sec. IV, we obtain numerical solutions for the self-similar solutions in the presence of the superfluid friction parameters α and α'. These solutions display a strong sensitivity to both initial conditions and the superfluid friction parameters. These solutions are classified as either singular or non-singular, depending on their behavior as time goes to infinity. The singular solutions can be used to construct vortex filament kinks, while the non-singular solutions can exhibit more exotic behavior. Finally, in Sec. V, we discuss various aspects of the solutions obtained. We also discuss why it is necessary to set the normal fluid velocity to zero for the self-similar filament solutions.

II. FORMULATION

If we consider the vortex to be aligned along the x axis (without loss of generality) to correspond with a normal fluid velocity oriented like $\mathbf{U} = U\mathbf{i}_x$, the LIA reduces to Ref. 13

$$\mathbf{v} = (1-\alpha')\gamma\kappa\mathbf{t} \times \mathbf{n} + \alpha\mathbf{t} \times \mathbf{U} + \alpha\gamma\kappa\mathbf{n} - \alpha' U\mathbf{t} + \alpha' U\mathbf{i}_x \, . \tag{2}$$

Assuming the deviations along the x axis to be sufficiently bounded in variation, we consider solutions $\mathbf{r} = x\mathbf{i}_x + y(x,t)\mathbf{i}_y + z(x,t)\mathbf{i}_z$. In particular, we do not allow vortex filaments to self-intersect, form and shed rings, or any such exotic behaviors which would yield non-uniqueness in the mathematical framework of the LIA. Such behaviors are best modeled through direct simulation of the governing Biot-Savart law, which is best done numerically for a fixed situation. In contrast, we shall be interested in exact analytical results, within the confines of the LIA. Note that this restriction also prevents the strong bending or twisting of a vortex back onto itself (so, the vortex filament

cannot cross or intersect itself, as mentioned above). Such types of solutions for the motion of a vortex filament have appeared in the literature. In all of these cases, the motion of the vortex filament is about one axis (here, we take the x-axis, without loss of generality). Hasimoto[14] considered planar vortex filaments and soliton solutions.[15] Kida[16] considered a number of types of vortex filament solutions. These solutions are in the curvature-torsion frame (the intrinsic frame of reference). In this paper, we shall instead focus on the extrinsic Cartesian reference frame, which is the natural geometry for the problem.

Various behaviors of solutions to the LIA for a vortex filament in superfluid ^{4}He have been observed in the literature. Van Gorder[17] determined the derivative nonlinear Schrödinger (NLS) equation resulting from the LIA (2), in the extrinsic Cartesian coordinate frame of reference, assuming motion of the filament about the x-axis (which permits complex potential form of the derivative NLS equation). This was in analogy to similar results for the standard fluid LIA, under the Cartesian frame.[18,19] This model is true to the nonlinear form of (2), thereby preserving the inherent nonlinear effects on the vortex filament solution. In (2), using the relations

$$\mathbf{v}=\frac{d\mathbf{r}}{dt}=y_t\mathbf{i}_y+z_t\mathbf{i}_z\,,\qquad \mathbf{t}=\frac{d\mathbf{r}}{ds}=\left(\mathbf{i}_x+y_x\mathbf{i}_y+z_x\mathbf{i}_z\right)\frac{dx}{ds}\,,\qquad \frac{dx}{ds}=\frac{1}{\sqrt{1+y_x^2+z_x^2}}\,,$$

$$\begin{aligned}\kappa\mathbf{n}=&-(y_xy_{xx}+z_xz_{xx})\frac{dx}{ds}\mathbf{i}_x+\left(y_{xx}\frac{dx}{ds}-(y_x^2y_{xx}+y_xz_xz_{xx})\right)\frac{dx}{ds}\mathbf{i}_y\\&+\left(z_{xx}\frac{dx}{ds}-(z_xy_xy_{xx}+z_x^2z_{xx})\right)\frac{dx}{ds}\mathbf{i}_z\,,\end{aligned}$$

and making the change of dependent variable in terms of the complex potential function

$$\Phi(x,t)=y(x,t)+iz(x,t)\,,$$

we find that the potential form of the LIA which includes superfluid friction parameters is given by

$$i\Phi_t+\frac{\alpha'Ui\Phi_x}{(1+|\Phi_x|^2)^{1/2}}-\frac{\alpha\gamma i\Phi_{xx}}{(1+|\Phi_x|^2)^2}-\alpha U\Phi_x+\frac{(1+\alpha')\gamma\Phi_{xx}}{(1+|\Phi_x|^2)^{3/2}}=0\,.\tag{3}$$

In general, the nonlinear equation (3) does not admit a self-similar solution (as may be verified; we revisit this point later in Sec. V). However, in the slightly less general case of $U=0$, we have a similarity solution. While this may seem excessively restricting, note that superfluid turbulence in the absence of a normal-fluid component is still of physical relevance.[21] It has been shown that bundle reconnections are possible (at temperature 1.65 K) in the case where the normal fluid velocity is zero.[22] Actually, the $U=0$ limit corresponds to the low temperature limit, where there is physically little or no normal fluid influence.[23] Later, we shall discuss a way by which we may include the case of non-zero normal fluid velocity. To do so, we will transform the self-similar solution into a new solution, which breaks the self-similarity at larger time scales.

To see this, we introduce what can be verified as being a unique (up to multiplicative scaling) similarity transformation

$$\Phi(x,t)=\sqrt{\gamma t}f(\eta),\tag{4}$$

where $\eta=\frac{x}{\sqrt{\gamma t}}$. Despite the reduction $U=0$, this solution still takes into account the superfluid friction parameters α and α', and hence is still of relevance. Invoking the similarity transformation (4), we obtain from (3) the ordinary differential equation

$$\frac{i}{2}\left(f-\eta f'\right)+\left(\frac{1+\alpha'}{\left(1+|f'|^2\right)^{3/2}}-i\frac{\alpha}{\left(1+|f'|^2\right)^2}\right)f''=0\,,\tag{5}$$

where prime denotes differentiation with respect to η. Next, writing $f(\eta)$ in the form

$$f(\eta)=R(\eta)\exp\left(i\Theta(\eta)\right)\,,\tag{6}$$

we obtain the coupled system

$$\frac{\eta}{2}R\Theta' + (1+\alpha')\frac{R'' - R\Theta'^2}{\left(1+R^2\Theta'^2+R'^2\right)^{3/2}} + \alpha\frac{R\Theta'' - 2R'\Theta'}{\left(1+R^2\Theta'^2+R'^2\right)^{2}} = 0\,, \tag{7}$$

$$\frac{1}{2}\left(R-\eta R'\right) + (1+\alpha')\frac{R\Theta'' - 2R'\Theta'}{\left(1+R^2\Theta'^2+R'^2\right)^{3/2}} - \alpha\frac{R'' - R\Theta'^2}{\left(1+R^2\Theta'^2+R'^2\right)^{2}} = 0\,. \tag{8}$$

For space-time variables $(x,\ t)$, solutions can be plotted in the Cartesian reference frame $\mathbf{r} = (x, y, z)$ given by

$$\mathbf{r} = \left(x,\ \sqrt{\gamma t}R\left(\frac{x}{\sqrt{\gamma t}}\right)\cos\left(\Theta\left(\frac{x}{\sqrt{\gamma t}}\right)\right),\ \sqrt{\gamma t}R\left(\frac{x}{\sqrt{\gamma t}}\right)\sin\left(\Theta\left(\frac{x}{\sqrt{\gamma t}}\right)\right)\right)\,. \tag{9}$$

III. ANALYTICAL PROPERTIES IN THE $\alpha, \alpha' \to 0$ LIMIT

The behavior of solutions to the standard and superfluid models are qualitatively similar, with quantitative differences arising from the inclusion of the superfluid friction parameters. To recover the standard fluid case, we set $\alpha = \alpha' = 0$ in (7) and (8) to obtain

$$\frac{\eta}{2}R\Theta' + \frac{R'' - R\Theta'^2}{\left(1+R^2\Theta'^2+R'^2\right)^{3/2}} = 0\,, \qquad \frac{1}{2}\left(R-\eta R'\right) + \frac{R\Theta'' - 2R'\Theta'}{\left(1+R^2\Theta'^2+R'^2\right)^{3/2}} = 0\,. \tag{10}$$

Since the standard and superfluid solutions are qualitatively similar (since the derivative NLS equation arising from the superfluid case is a type of structural perturbation of the derivative NLS equation arising from the standard fluid case), and since the standard fluid equations are amenable to analysis, we shall consider analytical properties of self-similar solutions governed by (10).

We should note that self-similar solutions in the case where $U = 0$ have been studied previously. Lipniacki[9,10] has studied such self-similar solutions in the intrinsic formulation of the LIA (the curvature-torsion frame). Svistunov[12] obtained a formulation for Cartesian frame in the temperature zero limit, corresponding to the $\alpha, \alpha' \to 0$ limit.

A. Constant phase solution yielding a linear filament

In the special case where the phase is constant, say $\Theta(\eta) = \Theta_0$, we obtain the equations $R'' = 0$ and $R - \eta R' = 0$. These equations are satisfied only for $R(\eta) = C\eta$, where C is an arbitrary scaling constant. As such, we recover

$$f(\eta) = Ce^{i\Theta_0}\eta = (C_1 + iC_2)\eta\,, \tag{11}$$

for appropriate real-valued constants C_1 and C_2. Mapping back to $\Phi(x, t)$, we have

$$\Phi(x,t) = \sqrt{\gamma t}(C_1 + iC_2)\frac{x}{\sqrt{\gamma t}} = (C_1 + iC_2)x\,, \tag{12}$$

hence $y(x,\ t) = C_1 x$ and $z(x,\ t) = C_2 x$. With this, we have shown that any constant phase solution must be linear in x and constant in t. Note that this case corresponds to $R(0) = 0$. Physically, this solution corresponds to the unperturbed line filament $\mathbf{r} = (x, C_1 x, c_2 x)$.

B. Non-constant phase as a function of amplitude

From the form of (10), it is clear that the phase Θ and amplitude R of a solution (6) are strongly coupled. From (10), we find

$$\frac{\frac{\eta}{2}R\Theta'}{R'' - R\Theta'^2} = -\frac{1}{\left(1+R^2\Theta'^2+R'^2\right)^{3/2}} = \frac{\frac{1}{2}\left(R-\eta R'\right)}{R\Theta'' - 2R'\Theta'}\,. \tag{13}$$

Note that the middle term in (13) is always negative and finite (for any real-valued R and Θ), and hence so are the left and right terms. Setting the left and right hand sides equal, and then manipulating the resulting equation (including multiplying the final expression by 2η), we have

$$2\eta^2 R^2\Theta'\Theta'' - 6\eta^2 R R'\Theta'^2 + 2\eta R^2\Theta'^2 = 2\eta(R-\eta R')R''\,. \tag{14}$$

Observe that the left hand side of (14) is nearly a total derivative. Indeed, we find that (14) is equivalent to

$$R^8\frac{d}{d\eta}\left\{\eta^2\Theta'^2R^{-6}\right\} = 2\eta(R-\eta R')R''\,. \tag{15}$$

Cross multiplying and integrating, we obtain

$$\eta^2\Theta'^2R^{-6} = \int_0^\eta \frac{2\xi(R(\xi)-\xi R'(\xi))R''(\xi)}{R^8(\xi)}d\xi\,. \tag{16}$$

Solving Eq. (16) for Θ'^2 gives

$$\Theta'^2 = \frac{R^6(\eta)}{\eta^2}\int_0^\eta \frac{2\xi(R(\xi)-\xi R'(\xi))R''(\xi)}{R^8(\xi)}d\xi\,, \tag{17}$$

which is an exact relation for the change of the phase Θ (in η) as a function of the amplitude R and its derivatives. We then have the local representation

$$\Theta(\eta) = \Theta_0 + \int_0^\eta \Theta'(\xi)d\xi = \Theta_0 + \int_0^\eta \sqrt{\frac{R^6(\xi)}{\xi^2}\int_0^\xi \frac{2\zeta(R(\zeta)-\zeta R'(\zeta))R''(\zeta)}{R^8(\zeta)}d\zeta}\,d\xi\,. \tag{18}$$

For small η, we write $R(\eta) = R(0) + R'(0)\eta + \frac{R''(0)}{2}\eta^2 + O(\eta^3)$, so (18) becomes

$$\Theta(\eta) \approx \Theta_0 + \int_0^\eta \sqrt{\frac{R(0)^6}{\xi^2}\int_0^\xi \frac{2\zeta R''(0)}{R(0)^7}d\zeta}\,d\xi = \Theta_0 + \int_0^\eta \sqrt{\frac{R''(0)}{R(0)}}d\xi = \Theta_0 + \sqrt{\frac{R''(0)}{R(0)}}\eta\,. \tag{19}$$

Since this holds true in the small-η regime, it is clear, then, that

$$\Theta'(0) = \sqrt{\frac{R''(0)}{R(0)}}\,. \tag{20}$$

Hence, the initial data $R''(0)$, $R(0)$, and $\Theta'(0)$ are closely related. In particular, when $R(0)\neq 0$, this relation allows us to determine $R''(0)$ in terms of $R(0)$ and $\Theta'(0)$ alone. While this follows from (19), it could have also been obtained from setting $\eta = 0$ in Eq. (10). As such, we see that the local solution (18) is consistent with the system (10). Likewise, from (10), we can determine $\Theta''(0)$ as

$$\Theta''(0) = 2\frac{\Theta'(0)R'(0)}{R(0)} - 2\left(1 + R(0)^2\Theta'(0)^2 + R'(0)^2\right)^{3/2}\,, \tag{21}$$

and making use of (20), we see that $\Theta''(0)$ can be completely described in terms of R and its derivative at $\eta = 0$, to wit

$$\Theta''(0) = 2\frac{R'(0)\sqrt{R''(0)/R(0)}}{R(0)} - 2\left(1 + R(0)R''(0) + R'(0)^2\right)^{3/2}\,. \tag{22}$$

Therefore, we can completely determine the curvature of a filament at the origin $\eta = 0$ in terms of the initial data $R(0)$, $R'(0)$, $\Theta(0)$, and $\Theta'(0)$.

C. Constant modulus solution $R(\eta) = R_0$

Let us now consider the case where $f(\eta) = R_0\exp(i\Theta(\eta))$, a constant modulus solution to (5). (Of course, we pick $R_0 > 0$ to avoid the zero solution.) Equation (14) then reduces to

$$2\eta(\eta\Theta'' + \Theta') = 0\,, \tag{23}$$

which admits a solution

$$\Theta(\eta) = \Theta_0 + C\ln(|\eta|) \tag{24}$$

for $\eta \neq 0$. So, a constant amplitude solution f takes the form

$$f(\eta) = R_0 \exp(i\Theta_0 + iC\ln(|\eta|)) = R_0\cos(\Theta_0 + C\ln(|\eta|)) + iR_0\sin(\Theta_0 + C\ln(|\eta|))\,. \tag{25}$$

The $R(\eta) = R_0$ solution then corresponds to a filament of the form

$$\mathbf{r} = \left(x,\, R_0\sqrt{\gamma t}\cos\left(\Theta_0 + C\ln\left|\frac{x}{\sqrt{\gamma t}}\right|\right),\, R_0\sqrt{\gamma t}\sin\left(\Theta_0 + C\ln\left|\frac{x}{\sqrt{\gamma t}}\right|\right)\right). \tag{26}$$

D. Small oscillation solutions

The obtained self-similar solution $f(\eta)$ scales as a linear function of η for large η. About this linear function appear oscillations, and in the present section we shall attempt to describe this behavior analytically. Let us assume a solution of the form

$$f(\eta) = q\eta + Ag(\eta)\,, \tag{27}$$

where q is the coefficient of the linear dominating term for $|\eta| \to \infty$, $g(\eta)$ is the function holding the deviations from this linear function (in particular, the oscillations), and A the maximal magnitude of the deviations. As seen in the numerical simulations, the deviations are small. So, it makes quantitative sense to consider A as a perturbation parameter. Assuming a solution of the form

$$g(\eta) = g_0(\eta) + Ag_1(\eta) + O(A^2)\,, \tag{28}$$

we find

$$\frac{i}{2}(g_0 - \eta g_0') + \frac{1}{(1+q)^{3/2}}g_0'' = 0\,, \tag{29}$$

$$\frac{i}{2}(g_1 - \eta g_1') + \frac{1}{(1+q)^{3/2}}g_1'' = \frac{3}{2(1+q)^{5/2}}(g_0 + g_0^*)g_0''\,. \tag{30}$$

To solve (29), let us make the substitution $G(\eta) = g_0(\eta) - \eta g_0'(\eta)$, which reduces (29) to

$$G'(\eta) = \frac{i}{2}(1+q)^{3/2}\eta G(\eta)\,, \tag{31}$$

hence

$$G(\eta) = \exp\left(\frac{i}{4}(1+q)^{3/2}\eta^2 + c_0\right). \tag{32}$$

Then $G(\eta) = g_0(\eta) - \eta g_0'(\eta)$ yields the solution

$$\begin{aligned} g_0(\eta) &= c_1\eta + c_2\eta\int^{\eta}\frac{1}{\xi^2}\exp\left(\frac{i}{4}(1+q)^{3/2}\xi^2\right)d\xi \\ &= \left\{c_1 - c_2\sqrt{i}\frac{\sqrt{\pi}}{2}\mathrm{erfi}\left(\frac{\sqrt{i}}{2}(1+q)^{3/4}\eta\right) - \frac{c_2}{\eta}\exp\left(\frac{i}{4}(1+q)^{3/2}\eta^2\right)\right\}\eta\,. \end{aligned} \tag{33}$$

Since we want only the oscillatory contribution as $\eta \to \infty$, we compute the asymptotics

$$\begin{aligned} g_0(\eta) = &\left(c_1 + \frac{\sqrt{-i\pi}}{2}c_2\right)\eta \\ &+ \exp\left(\frac{i}{4}(1+q)^{3/2}\eta^2\right)\left\{-\left(1 + (1+q)^{3/4}\right)c_2 + \frac{2ic_2}{(1+q)^{9/4}}\frac{1}{\eta^2} + O\left(\frac{1}{\eta^4}\right)\right\}. \end{aligned} \tag{34}$$

Picking $c_1 = -\sqrt{-i\pi}c_2/2$, we remove the linear growth term. The constant c_2 becomes a scaling, so we take $c_2 = 2/\sqrt{i\pi}\hat{c}(q)$ (where $\hat{c}(q)$ is a scaling factor) to simplify the resulting expression, obtaining

$$g_0(\eta) = \hat{c}(q)\left\{i - \text{erfi}\left(\frac{\sqrt{i}}{2}(1+q)^{3/4}\eta\right)\right\}\eta - \hat{c}(q)\sqrt{\frac{2}{\pi}}(1-i)\exp\left(\frac{i}{4}(1+q)^{3/2}\eta^2\right). \quad (35)$$

Observe that the linear growth rate, q, of these solutions strongly influences the manner of oscillation. Picking $\hat{c}(q)$ appropriately, the function $g_0(\eta)$ has maximal modulus equal to unity.

Using this perturbation result, up to order $O(A^2)$ we have that the vortex filament is described by

$$\begin{aligned}\mathbf{r} &= \left(x, \sqrt{\gamma t}\ \text{Re}\ g_0(\eta), \sqrt{\gamma t}\ \text{Im}\ g_0(\eta)\right)\\ &= (1, \text{Re}\ q, \text{Im}\ q)\,x + \left(0, \text{Re}\ g_0\left(\frac{x}{\sqrt{\gamma t}}\right), \text{Im}\ g_0\left(\frac{x}{\sqrt{\gamma t}}\right)\right)A\sqrt{\gamma t} + O(A^2).\end{aligned} \quad (36)$$

In order to get a better feeling for the oscillations, let us take $q = 0$ to remove the linear trend. Then we obtain

$$\mathbf{r} = \left(x, A\sqrt{\gamma t}\ \text{Re}\ g_0\left(\frac{x}{\sqrt{\gamma t}}\right), A\sqrt{\gamma t}\ \text{Im}\ g_0\left(\frac{x}{\sqrt{\gamma t}}\right)\right) + O(A^2). \quad (37)$$

Taking $q = 0$, we see that $|g_0(\eta)| \leq |g_0(0)|$ for all $\eta \geq 0$. So, to normalize our expression, we take $\hat{c}(0) = 1/g_0(0) = \sqrt{2\pi}(1+i)/4$. Then

$$g_0(\eta) = \frac{\sqrt{2\pi}(1+i)}{4}\left\{i - \text{erfi}\left(\frac{\sqrt{i}}{2}(1+q)^{3/4}\eta\right)\right\}\eta - \exp\left(\frac{i}{4}(1+q)^{3/2}\eta^2\right) \quad (38)$$

and $g_0(\eta)$ has maximum modulus equal to unity on $\eta \geq 0$. Replacing $\eta = x/\sqrt{\gamma t}$, we can plot the similarity solution (37), and we do so in Figure 1. Note that we have scaled the solution so that $A = 1$ in the latter two components, since we are only interested in the qualitative shape of the vortex filament at this juncture.

E. Asymptotic solution for large η

Let us consider the asymptotics for the singular solution. We substitute $R(\eta) = \eta^{-1}r(\eta)$, and keeping highest order contributions in (10) η (that is, we discard terms of order $O(\eta^{-2})$) we find

$$r'' + \frac{\eta}{2}r\Theta - r\Theta'^2 = 0 \qquad \text{and} \qquad r\Theta'' - \left(\frac{\eta}{2} + 2\Theta'\right)r' + r = 0. \quad (39)$$

Defining $\zeta = r'/r$ and $\xi = \Theta'$, we have the coupled system of first order differential equations

$$\zeta' + \zeta^2 + \left(\frac{\eta}{2} - \xi\right)\xi = 0 \qquad \text{and} \qquad \xi' - 2\zeta\xi - \frac{\eta}{2}\zeta + 1 = 0. \quad (40)$$

We find the solution $\zeta(\eta) = 1/\eta$ and $\xi(\eta) = \eta/2$. Then, $r(\eta) = r_0\eta$ so $R(\eta) = r_0$, a constant. Meanwhile, $\Theta(\eta) = \Theta_0 + \eta^2/4$. So, in the large η limit, we have $f(\eta) = r_0 e^{i\Theta_0}\exp(i\eta^2/4)$. Picking $\Theta_0 = 0$, we have $f(\eta) = r_0\cos(\eta^2/4) + ir_0\sin(\eta^2/4)$. The solution in the large η regime is then given as

$$\mathbf{r} = \left(x, r_0\sqrt{\gamma t}\cos\left(\frac{x^2}{4\gamma t}\right), r_0\sqrt{\gamma t}\sin\left(\frac{x^2}{4\gamma t}\right)\right). \quad (41)$$

Note that this solution is in complete agreement with the complex exponential term which gives oscillations to the small-amplitude solution (38). This makes complete sense for the present case, as the solutions tend toward pure oscillations for large magnitudes $|\eta|$. Hence, this asymptotic result agrees completely with the large η limit of the small-amplitude case when the linear trend is removed. We shall see that this also agrees with the numerical solutions presented in Sec. IV.

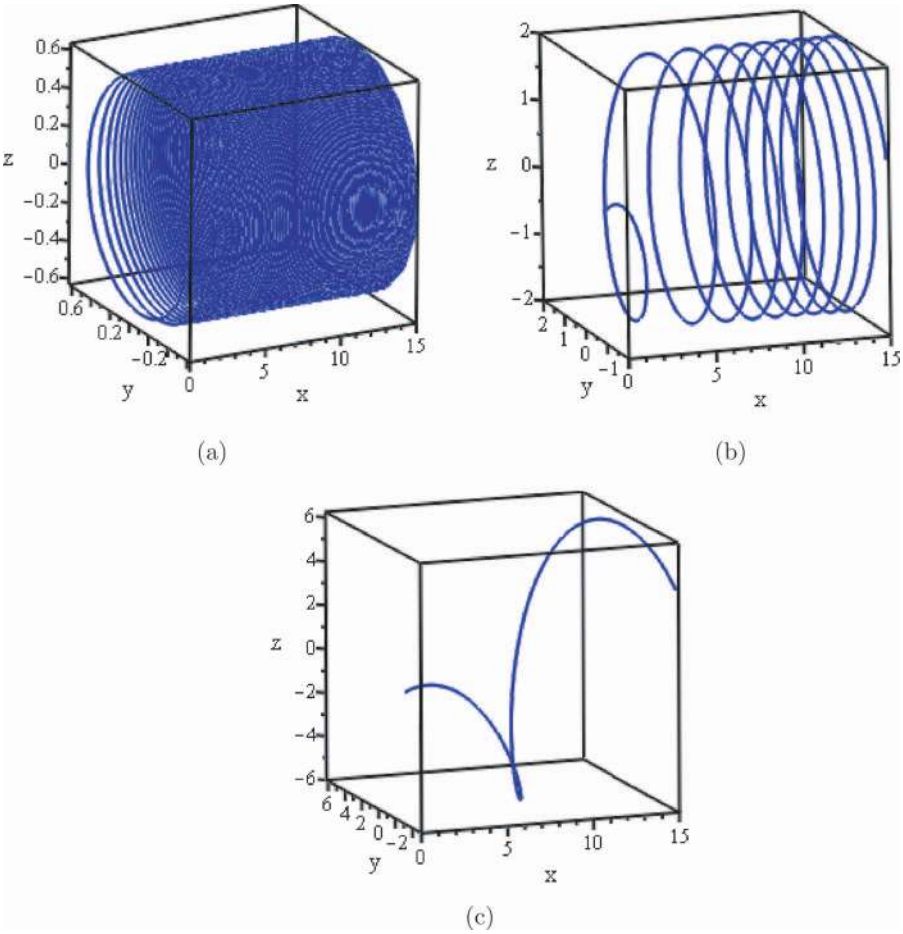

FIG. 1. Plot of small-amplitude solutions (37) corresponding to (38) over space $x \in [0, 15]$ given (a) $t = 0.1$, (b) $t = 1$, and (c) $t = 10$. We fix $\gamma = 1$; changes in γ would simply manifest as a dilation of the temporal variable t, thereby altering (up to a scale) the temporal variation shown in (a)–(c).

IV. NUMERICAL SIMULATIONS

At this point, we solve the transformed version of the LIA (7) and (8). Instead of using (9), however, note that if we consider the transformed coordinate system (η, τ) in place of (x, t), where η is the similarity variable and τ is the transformed time $\tau = \sqrt{\gamma t}$ (under which η reads $\eta = x/\tau$), we have the simpler expression

$$\hat{\mathbf{r}} = (\eta, R(\eta)\cos\Theta(\eta), R(\eta)\sin\Theta(\eta)), \tag{42}$$

where $\hat{\mathbf{r}} = \mathbf{r}/\tau$ is the time-normalized position vector. Thus, through a numerical simulation of solutions $R(\eta)$ and $\Theta(\eta)$ to (7) and (8), we can recover the vortex structure $\hat{\mathbf{r}}$ for the superfluid ^{4}He case (and, if need be, convert the results back to the original coordinates (x, t)). We shall therefore obtain numerical solutions to (7) and (8) and plot them in the natural coordinates (42).

The influence of the superfluid friction parameters α and α' will be of most interest, since these were excluded from the analytical results. Although the superfluid friction parameters are small, as we shall demonstrate, they are certainly not negligible.

Before we begin, let us take a look at the linearized system. We find that (7) and (8) has a linearized form

$$\begin{bmatrix} 1+\alpha' & \alpha R \\ -\alpha & 1+\alpha R \end{bmatrix} \begin{bmatrix} R'' \\ \Theta'' \end{bmatrix} + M(R, R', \Theta, \Theta') = 0, \tag{43}$$

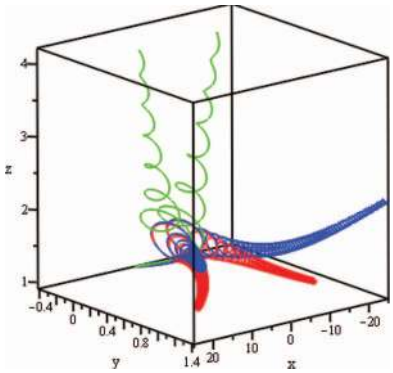

FIG. 2. Plot of singular self-similar solutions $\hat{\mathbf{r}}$ for (7) and (8). The red (lower) solution denotes $(\alpha, \alpha') = (0, 0)$, the blue (middle) solution denotes $(\alpha, \alpha') = (0.005, 0.003)$, and the green (upper) solution denotes $(\alpha, \alpha') = (0.073, 0.018)$. Here, $R(0) = 1$, $R'(0) = \Theta'(0) = 0$, $\Theta(0) = 2$.

where M is a vector with entries consisting of R, R', Θ, and Θ'. We see that

$$\det\begin{bmatrix} 1+\alpha' & \alpha R \\ -\alpha & 1+\alpha R \end{bmatrix} = [\alpha^2 + (1+\alpha')^2]R\,, \tag{44}$$

so the system is non-degenerate for all α and α', provided that $R \neq 0$. If, however, $R = 0$ (for instance, if we invoke the initial condition $R(0) = 0$), then the linearized system (43) for the nonlinear system (7) and (8) becomes degenerate. This must be taken into consideration as we proceed, when we desire solutions satisfying $R(0) = 0$, as this condition is needed for the non-singular solutions.

A. Singular solutions $R(0) > 0$

The first order of business is calibrating initial conditions. We should take $R(0) > 0$ for singular solutions, but the remaining three conditions can be selected somewhat arbitrarily. We therefore take $R(0) = 1$ for the singular solutions, so that solutions become singular in the $t \to \infty$ limit.

In Figure 2, we provide solutions which oscillate for small η and in the limit $\eta \to \pm\infty$ tend toward a line. The solutions satisfy $R'(0) = \Theta'(0) = 0$ and $\Theta(0) = 2$. These are kink-solutions: at $\eta = 0$ they alter their position (turning in the reverse direction). Note that the solutions are very sensitive to the superfluid friction parameters. Both the $(\alpha, \alpha') = (0, 0)$ and $(\alpha, \alpha') = (0.005, 0.003)$ cases give rapid oscillations near the origin, yet they diverge from one another, with the filaments ending up with drastically different orientations. Meanwhile, for the $(\alpha, \alpha') = (0.073, 0.018)$ case, the solutions oscillate far less rapidly and the vortex filament rapidly diverges from the other two cases. Note that, in the small α, α' limit, the numerical results agree well with the analytical formula (19). In particular, note that for small η, the phase is accurately approximated by (19). On the other hand, in the large η case, the numerical solutions agree well with the asymptotic formula (41).

The difference in these three vortex filaments lies in the behavior of $R(\eta)$. To demonstrate this, we plot $R(\eta)$ and $\Theta(\eta)$ in Figure 3, for each parameter set in Figure 2. Again, we see the small η agreement with the formula (19) and the large η agreement with the asymptotic formula (41). Compare these solutions with Figures 3 and 4 of Ref. 9, where relatively large values of the superfluid friction parameters were taken. For large values of α, the oscillations along the mean curve die off, leaving a V-shaped filament. As α is made progressively closer to zero, the oscillations increase in frequency, yielding the behavior we see in Figure 2. In the curvature-torsion model studied by Lipniacki,[9,10] the filament becomes more wavy as α is decreased toward zero.

B. Non-singular solutions $R(0) = 0$

For the non-singular solutions, we require $R(0) = 0$ so that $\lim_{t\to\infty} |\sqrt{\gamma t}\, f(x/\sqrt{\gamma t})| < \infty$. That is, so that $\|(y(x, t), z(x, t))\| < \infty$ as $t \to \infty$. As shown previously, the linearized system (43) is

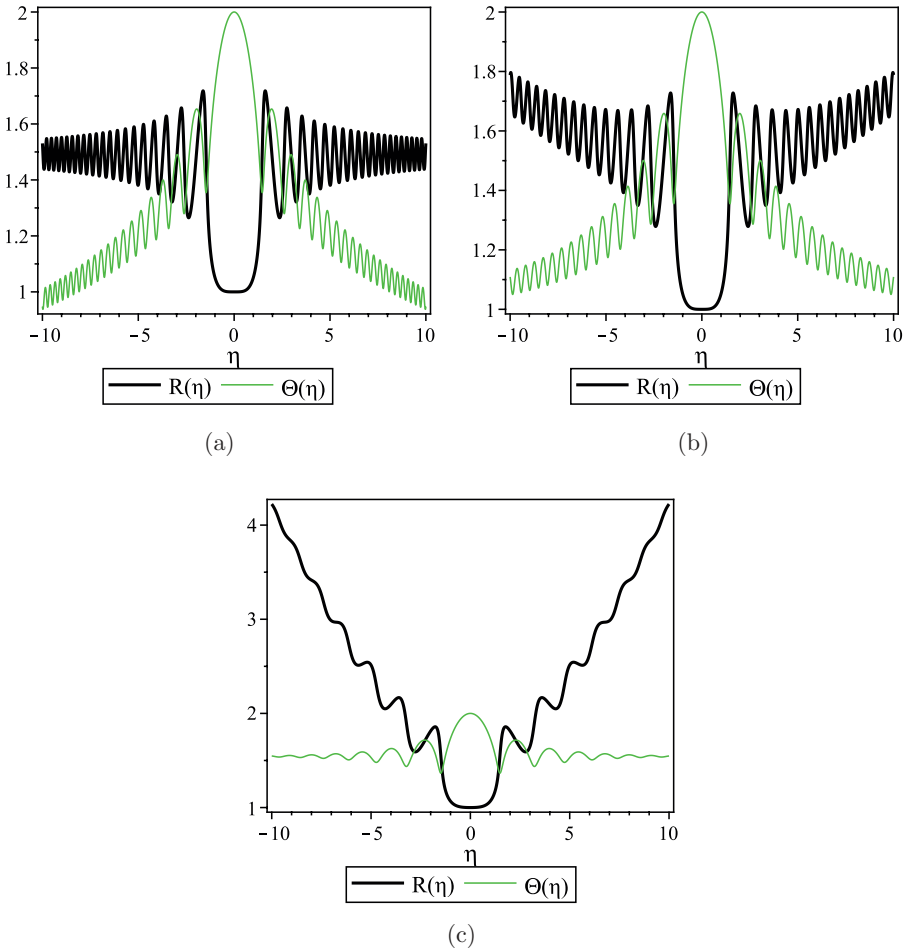

FIG. 3. Plot of self-similar solutions $R(\eta)$ and $\Theta(\eta)$ for (7) and (8) given (a) $(\alpha, \alpha') = (0, 0)$, (b) $(\alpha, \alpha') = (0.005, 0.003)$, and (c) $(\alpha, \alpha') = (0.073, 0.018)$. When the superfluid friction parameters are zero, the solution $R(\eta)$ oscillates about a fixed point. Yet, with the addition as even small superfluid friction parameters, the solution $R \to \infty$ as $|\eta| \to \infty$. Here, $R(0) = 1$, $R'(0) = \Theta'(0) = 0$, $\Theta(0) = 2$.

degenerate at $R = 0$, which will naturally complicate the numerical solution for the non-singular case since the needed initial condition results in such a degeneracy. To get around this, we introduce a slight perturbation $0 < \epsilon \ll 1$ so that $R(0) = \epsilon$. This will permit us to approximate the non-singular vortex filament. We find that taking $\epsilon = 10^{-3}$ will suffice; for $\epsilon < 10^{-3}$, we notice no qualitative difference in the solutions. The other initial conditions are again taken to be $R'(0) = \Theta'(0) = 0$ and $\Theta(0) = 2$, which provides us with symmetric solutions.

In Figure 4, we plot the non-singular solutions for various values of the superfluid friction parameters. Note that these solutions appear similar to those in Figure 5 of Lipniacki.[9] The plots of Lipniacki appear more well-behaved, since $\alpha = 1$ is taken. Since α scales positively with temperature, this large value of α corresponds to warmer temperatures. Indeed, we see that for small $\alpha \ll 1$, the behavior of the solutions for the Cartesian model is similar: the solutions are bounded, and appear to have two attractive regions.

V. DISCUSSION

After a series of reasonable assumptions and transformations, we have reduced the fully nonlinear local induction approximation (1) for the motion of a vortex filament in superfluid ^{4}He derived

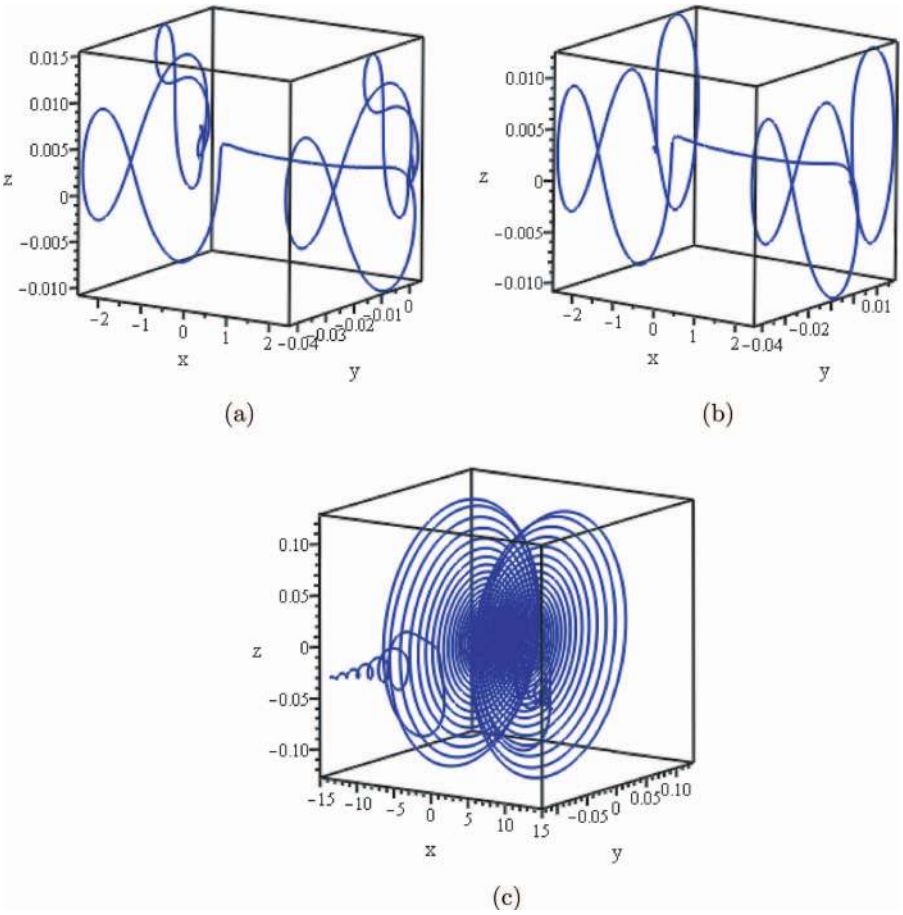

FIG. 4. Plot of non-singular self-similar solutions $\hat{\mathbf{r}}$ for (7) and (8) given (a) $(\alpha, \alpha') = (0, 0)$, (b) $(\alpha, \alpha') = (0.005, 0.003)$, and (c) $(\alpha, \alpha') = (0.073, 0.018)$. Here, $R(0) = \epsilon = 10^{-3}$, $R'(0) = \Theta'(0) = 0$, $\Theta(0) = 2$. Taking $\epsilon = 10^{-3}$ is sufficient to numerically approximate the non-singular vortex filament solution.

in Ref. 17 to an ordinary differential equation of the form

$$\frac{i}{2}\left(f - \eta f'\right) + \left(\frac{1+\alpha'}{\left(1+|f'|^2\right)^{3/2}} - i\frac{\alpha}{\left(1+|f'|^2\right)^{2}}\right) f'' = 0\,,$$

where $\eta = x/\sqrt{\gamma t}$ is a similarity variable. The vortex filament in the Cartesian frame is then given by

$$\mathbf{r} = \left(x, \sqrt{\gamma t}\ \mathrm{Re}\ f(\eta), \sqrt{\gamma t}\ \mathrm{Im}\ f(\eta)\right)\,.$$

From this formulation of the self-similar solution, we have been able to study various properties of the resulting vortex filament. Analytical solutions have been considered for the $\alpha, \alpha' \to 0$ regime, which is the limit under which the superfluid model reduces to the standard fluid model. In this case, we have been able to study the filament solutions in a qualitative manner. Of course, in order to determine the influence of superfluid friction parameters on the self-similar solutions, we need to consider numerical simulations. These simulations demonstrate the existence of two classes of solutions, depending on whether the solution is singular or not. (A singular solution is one in which $f(0) \neq 0$, since this implies that the limit $\sqrt{\gamma t}\, f(x/\sqrt{\gamma t})$ is unbounded as $t \to \infty$.)

A. Analytical results

The results corresponding to the α, $\alpha' \to 0$ limit were discussed in Sec. III, and effectively describe self-similar solutions to the Cartesian form of the LIA for a standard fluid. This model was previously considered in Refs. 18 and 19 where planar and helical vortex filaments were obtained by Van Gorder; see also Ref. 20. The self-similar solutions obtained here are distinct from those solutions. In Sec. III, we were able to determine that solutions grow linearly in η, the similarity variable. The solutions are shown to oscillate about a linear curve of the form $\mathbf{s} = (\eta, A\eta, B\eta)$. Note that $\mathbf{s}$ is the form of a constant-phase solution ($\Theta(\eta) = \Theta_0$). For the non-constant phase solutions, an elegant representation for the phase $\Theta(\eta)$ has been given in terms of the amplitude $R(\eta)$

$$\Theta(\eta) = \Theta_0 + \int_0^{\eta} \sqrt{\frac{R^6(\xi)}{\xi^2} \int_0^{\xi} \frac{2\zeta(R(\zeta) - \zeta R'(\zeta))R''(\zeta)}{R^8(\zeta)} d\zeta\, d\xi}\,.$$

In this case, we also find that the boundary data are related like $\Theta'(0) = \sqrt{R''(0)/R(0)}$.

The case of small-amplitude oscillations was considered perturbatively, and an analytic form of the oscillations (with the linear trend removed) was given to order $O(A)$, where A is the bound on the amplitude of the oscillations. We prove that the oscillations should go as

$$\exp\left(\frac{i}{4}(1+q)^{3/2}\eta^2\right)$$

once the linear trend is removed. While this analytic form of the oscillations was given in the α, α' $\to 0$ limit, it agrees completely with what we see in the numerics for the $\alpha \neq 0$, $\alpha' \neq 0$ case.

In order to better understand this behavior, we consider an asymptotic approximation of the solution in the $\eta \to +\infty$ limit. The resulting asymptotic solutions (with linear trend removed) take the form

$$\mathbf{r} = \left(x, r_0\sqrt{\gamma t}\cos\left(\frac{x^2}{4\gamma t}\right), r_0\sqrt{\gamma t}\sin\left(\frac{x^2}{4\gamma t}\right)\right),$$

which is in complete agreement with the $O(A)$ perturbation result.

B. Numerical results

While our numerical study is far from exhaustive, we have shown that the solution to the system (7) and (8) is very sensitive to the values of the superfluid friction parameters α and α'. Furthermore, in the case of singular solutions (those solutions with $R(\eta) > 0$ as $\eta \to 0^+$, the normalized filament tends infinitely far from the origin as $\eta \to \pm\infty$. In other words, $\|\hat{\mathbf{r}}\| \to \infty$ as $\eta \to \pm\infty$ for the singular solutions. For the non-singular solutions (those solutions with $R \to 0$ as $\eta \to 0^+$), we observe that $\|(y(x,t), z(x,t))\| < \infty$ as $\eta \to \pm\infty$. Hence, the non-singular solutions are bounded for all η.

We thus recover singular solutions, which grow as x becomes large, when $f(0) \neq 0$. Kink-type solutions fall within this class.[11] Such solutions are strongly influenced by the values of the superfluid friction parameters. Even a small increase in the superfluid friction parameters can lead to a drastic increase in where the filament is positioned at large x. These are the solutions which agree qualitatively well with the analytical solutions in the α, $\alpha' \to 0$ limit. The difference in parametric values of α and α' influences orientation as $x \to \pm\infty$ and in the frequency of oscillations. In particular, as α and α' increase, the frequency of oscillations diminishes, owing to the increased friction and hence energy loss.

On the other hand, we recover a second class of solutions when $f(0) = 0$. For any fixed x, this class of solutions remains bounded for all time. These solutions are of small magnitude, and exhibit more exotic forms of oscillations than do the singular solutions: the solutions exhibit small oscillatory excitations at some small positive value of η, before decaying back down toward zero. Such solutions are effectively small excitations of the solution $\mathbf{r} = (x, 0, 0)$. Note that when α and α' are sufficiently large (such as in the $T = 1.5$ K case), these solutions appear very similar in form

to a class of solutions obtained by Lipniacki,[10] though those solutions were obtained in a different manner than the solutions presented here.

Note that, in principle, there exists a correspondence between the curvature-torsion solutions and the Cartesian solutions discussed here. Going from the Cartesian frame to the curvature-torsion frame is relatively straightforward, since the curvature and torsion along an arc length element can be calculated directly in terms of the Cartesian solutions. Going in the reverse direction is more complicated. There is an additional frame, the tangent-arc length frame proposed by Umeki,[25] which can be seen as a natural bridge between the two. Mapping from the curvature-torsion frame into the tangent-arc length frame is more straightforward. Then, one may use the maps provided by Umeki[25] to connect the tangent-arc length frame solutions to Cartesian solutions. While the solutions are more complicated for the case where superfluid friction is considered (as opposed to the standard LIA), the transformations between the various coordinate frames are identical.

C. Self-similarity in other frames of reference

Solutions also exist in the literature for the arc length form of the LIA; helical solutions were previously obtained by Umeki[24,25] while planar vortex filaments were constructed by Van Gorder.[26] We are not aware of any self-similar solutions to the arc length formulation of the LIA for either a standard fluid or a superfluid. The arc length frame is one of two extrinsic real space frames (the other being the Cartesian frame discussed here). In the intrinsic frame, in particular the related torsion-curvature framework, Lipniacki[9] demonstrated the existence of self-similar solutions in a superfluid formulation of the LIA (retaining one of the superfluid friction parameters). As such, we find it likely that self-similar solutions are possible for the arc length form of the LIA for a superfluid.

Note that, for the Cartesian frame taken in the present paper, the similarity transform used for the superfluid was the same as that used for the regular fluid: $\Phi(x,t)=\sqrt{\gamma t}\, f(\eta)$ with $\eta = x/\sqrt{\gamma t}$. It makes sense, then, to determine whether the arc length form of the LIA for a standard fluid permits self-similar solutions. Recall[24,26] that the LIA in the arc length frame reads

$$i v_t + v_{ss} - \frac{2v^* v_s^2}{1+|v|^2} = 0\,, \tag{45}$$

where * denotes complex conjugation, $v(s,t) : \mathbb{R}\times(0,\infty)\to \mathbf{C}$, s is the arc length and t remains the time. The assumption $v(s,t)=g(\hat{\eta})$ where $\hat{\eta}=s/\sqrt{t}$ leads to a similarity solution, which is governed by the equation

$$-\frac{i}{2}\hat{\eta} g' + g'' - \frac{2g^* g'^2}{1+|g|^2} = 0\,. \tag{46}$$

Hence, the curvature-torsion form of the LIA, the Cartesian form of the LIA, and the arc length form of the LIA all share the same similarity transform, which is simply that of the heat equation: $\eta = x/\sqrt{t}$. The differences in the outer scaling factors (the t^ν factor in the similarity solution $t^\nu f(\eta)$) are dependent on the frame taken. Clearly, the appearance of self-similar solutions, such as those presented here, are intrinsic to the LIA and completely independent of the reference frame taken.

Owing to the rather simple representation for a planar filament in the arc length frame[26] compared to the more complicated result for the Cartesian frame,[20] it may be possible that some vortex filaments in superfluid ^{4}He may be more succinctly described in an arc length coordinate frame. The derivation of the Hall-Vinen model in the arc length frame will yield a generalization of (45), which shall account for superfluid friction parameters. This will be taken up in a subsequent work.

D. Destruction of similarity by a normal flow impinging on the vortex

In Sec. II, we mentioned that the normal fluid velocity must be zero in order to permit self-similarity; indeed, including terms with $U\Phi_x$ would remove the possibility of similarity for any transform $\Phi(x,t)=t^\nu f(xt^\beta)$. It is natural, then, to wonder what effect a small perturbation in U (i.e., $|U|\ll 1$) would have on destroying similarity. Assuming a solution (4) for (3) with $U\neq 0$, we find

that (5) becomes

$$\frac{i}{2}\left(f-\eta f'\right)+\left(\frac{1+\alpha'}{\left(1+|f'|^2\right)^{3/2}}-i\frac{\alpha}{\left(1+|f'|^2\right)^2}\right)f''+U\sqrt{\gamma t}\left\{\frac{\alpha'}{(1+|f'|^2)^{1/2}}-\alpha\right\}f'=0\,. \tag{47}$$

What this shows is that deviations from the self-similar solution, for even small yet fixed normal fluid velocity U, will deviate as $\sqrt{t}$ due to the addition of non-zero normal flow. Hence, the normal flow destroys the self-similarity. If we view the term with $U\sqrt{\gamma t}$ as a structural perturbation to Eq. (5), the perturbation grows with order $O(t^{1/2})$ in t. So, there is no reasonable way to view such a term as a small perturbation of the self-similar solution for all time, and similarity is destroyed with the introduction of $U\neq 0$.

With all of that said, there is a way to obtain solutions to the $U\neq 0$ problem, and, in fact, we can describe such solutions in terms of the similarity solutions already obtained in Secs. V A–V C. Consider the $\alpha>0$ and $\alpha'=0$ case (which is physically relevant and is considered in a number of studies. Instead of assuming a purely self-similar solution, let us consider a solution with a self-similar contribution that is allowed to drift in time. To that end, let us assume a solution

$$\Phi(x,t)=\sqrt{\gamma t}F(\sigma), \tag{48}$$

where $\sigma=\frac{x}{\sqrt{\gamma t}}-iw(t)=\eta-iw(t)$. Here, the new variable σ modifies the pure similarity variable η by adding a drift term $w(t)$ (which itself takes the form of a Wick rotation). Then, in the place of (47), we obtain

$$\frac{i}{2}\left(F-\sigma F'\right)+\left(\frac{1}{\left(1+|F'|^2\right)^{3/2}}-i\frac{\alpha}{\left(1+|F'|^2\right)^2}\right)F''=0\,, \tag{49}$$

where prime denotes differentiation with respect to σ, while $w(t)$ satisfies

$$w+2\gamma t\frac{dw}{dt}-2\alpha U\sqrt{\gamma t}=0\,. \tag{50}$$

The drift term must then read

$$w(t)=\frac{2\alpha U}{1+\gamma}\sqrt{\gamma t}\,. \tag{51}$$

Here, terms in the derivative Φ_t has cancelled the contribution of the form $2\alpha U\sqrt{\gamma t}\Phi_x$. Note that (49) is simply (5) under the replacement $f\to F$ and $\eta\to\sigma$. Hence, one may use the solutions derived above in order to obtain solutions to $F(\sigma)$.

We may use this new transformation to determine the asymptotic behavior of a solution $F(\sigma)$. Assume that $f(\eta)\approx r_0\exp(i\eta^2/4)$ asymptotically. Then, $F(\sigma)\approx r_0\exp(i\sigma^2/4)$ asymptotically, and hence $\Phi(x,t)$ goes as

$$\Phi(x,t)\approx r_0\sqrt{\gamma t}\exp\left(i\left[\frac{x^2}{4\gamma t}-\frac{\alpha^2U^2\gamma}{(1+\gamma)^2}t\right]\right)\exp\left(\frac{\alpha U}{1+\gamma}x\right) \tag{52}$$

asymptotically. Due to the fact that σ is the addition of a pure similarity variable and a Wick rotation of a scaling of time, the asymptotic properties of this solution differ in a subtle yet significant way from the $U=0$ case considered before. While the oscillatory behavior is still present in the asymptotic result, there is now a real-values exponential, which makes the filament arbitrarily large as $x\to\infty$. However, this is not inconsistent with the numerical results, where for the singular filaments, taking $\eta\to\infty$ yielded unbounded limits. Therefore, the addition of $U\neq 0$ has not altered the qualitative properties of the asymptotic behavior of the vortex filaments. However, it has modified the type of solution. Instead of pure self-similar solutions which are quasi-static, we obtain filaments which drift and deform at a rate depending on the strength of the normal fluid flow U.

The actual manner in which U influences the filament can be seen through two effects. First, there is a modification to the local behavior, such as the types of waves or oscillations which form along the vortex filament. Since there is now a term which scales as $\frac{\alpha^2U^2\gamma}{(1+\gamma)^2}t$ influencing the oscillations,

large time scales and small time scales have strong effects on the manner of oscillations. Previously, only small time scales had significant effects. The second effect is what we alluded to above. The manner of growth of the singular vortex filament away from the center axis of rotation was of the order $\sqrt{t}$ in the $U = 0$ case. Now, with the inclusion of $U \neq 0$, the growth rate is more accurately approximated by $\sqrt{\gamma t}\exp\left(\frac{\alpha U}{1+\gamma}x\right)$. Hence, there is now growth in space and time.

These modifications are completely consistent with what one might expect from (47). Indeed, in the limit where $t \ll 1$, the results obtained here are essentially the same as for the $U = 0$ case. So, the influence of the normal fluid on a similarity solution is felt at larger times, and the similarity breaks down for those times. The manner in which similarity is lost is best seen through the function $F(\sigma)$ and its asymptotics.

E. Physical implications

The solutions obtained (through both the asymptotic and the numerical results) are in agreement with the studies by Lipniacki[9,10] and Svistunov[12] in the $\alpha, \alpha' \to 0$ limit. What we have done here is show that self-similarity is still inherent in vortex solutions to the LIA, even when superfluid friction parameters are included. Hence, the Hall-Vinen formulation of vortex dynamics in superfluid ^{4}He admits self-similarity of solutions when there is no normal flow impinging on the vortex. Such a normal flow disrupts the vortex. Even when solutions do exist in the presence of normal flow impinging on the vortex, the resulting solutions do not maintain self-similarity. In other words, the behavior of the vortex filament may vary strongly with the size of the length scale. In the no normal fluid case, the self-similarity inherent in the obtained solutions physically implies that the solutions exhibit the same general behavior at arbitrary length scales.

While the addition of the superfluid friction parameters complicated the form of the nonlinear partial differential equation we must solve, including such terms is necessary, as we have seen from the numerical simulations that such parameters strongly influence the vortex filament solutions. Indeed, as was shown in Figures 2–4, rather drastic quantitative changes can appear given seemingly minor increases in the superfluid friction parameters. Since the parameters scale positively with temperature, what we have really done here is demonstrate the influence of temperature on the self-similar motion of a vortex filament in superfluid ^{4}He. As the temperature increases, the singular filaments take on a sharp V-shape (a kink-shape) toward the z axis. Furthermore, the waves or oscillations on these vortex filament solutions diminish for larger temperatures. In a way, this is in qualitative agreement with the finding in Ref. 28 that for multiple vortex filaments, the vortex tangle is smoother for positive temperatures than for the zero temperature case. For the non-singular solutions which are always bounded in distance from the axis of orientation, the solutions appear as excitations near the origin, and then tend toward the line filament $\mathbf{r} = (x, 0, 0)$ for larger x. The form of these local excitations depends strongly on the superfluid friction parameters.

Many of the numerical plots agree with the results for the curvature-torsion model studied by Lipniacki.[9,10] While many of the solutions are given for the "warm" case of $\alpha = 1$ (recall that α scales positively with temperature), many qualitative features remain. The singular solutions feature kinks near the origin. As the filament travels away from the origin on either side, the filament will develop waves or oscillations, depending on the size of the superfluid friction parameter α. Indeed, as α increases, the waves or oscillations tend to dissipate. On the other hand, the non-singular vortex filament solutions remain confined to a bounded region.

Since the Hall-Vinen model is an extension of the LIA which includes superfluid effects, it is natural to question whether the solutions are reasonable approximations to the non-local model governing the vortex filaments. This point was discussed by Lipniacki,[9] and it was argued that for increasing spatial scales, the similarity solutions are reasonable, whereas for decreasing spatial scales, the similarity solutions fail to be accurate representations of the true vortex filament motions, and nonlinear effects are needed. More accurate solutions in the decreasing scale case can be obtained through the simulation of a generalized Biot-Savart law which accounts for superfluid friction. The comments hold for the Cartesian case, as well.

Since the LIA, and therefore the Hall-Vinen model, are approximations to the true motion of vortex filaments, the degree to which these self-similar solutions approximate the true solutions is worth considering. In cases where the filaments are not tightly coiled, vortex filament interactions would involve local crossings. While the full Biot-Savart law is needed to understand arbitrary crossings, simple crossing can be approximated locally for this basic case.[20] For more complicated filaments, such as those with many waves or oscillations, or those featuring many loops (as is true of some of the non-singular vortex filaments), interactions may occur at a number of places, so LIA will not be as useful an approximation.

As remarked before, a normal fluid impinging on the vortex filament will destroy self-similarity. This does not mean that the solution is completely destroyed, only that it is modified. Indeed, the solution may simply be perturbed by some quantity. If this perturbation or excitation is small, it is likely that the solution can, more-or-less, maintain its form, modified only by a perturbation term. This would make sense in the context of the stability results of Banica and Vega,[27] who consider the standard ($\alpha = \alpha' = 0$) model under the curvature-torsion frame and determine that the kink-type similarity solutions are indeed stable under sufficiently small perturbations. While the proof for the $\alpha > 0, \alpha' > 0$ case has never been considered, it is reasonable that, under small enough perturbations and small enough superfluid friction parameters, the solutions will remain robust. For very large perturbations (i.e., large normal fluid velocity), the similarity solutions likely break down, but this is also physically reasonable.

As addressed in Subsection V D, if we introduce a new variable σ which shifts the similarity variable by a function of time alone, then we can study the influence of a normal fluid impinging on the solutions. What we find is that the similarity solutions are transformed into functions of this new variable. The greatest differences occur for large values of time, whereas for small time, the solutions are essentially the same as the purely self-similar ones. For large time, the singular solutions exhibit a faster rate of growth away from the central axis along which the vortex is aligned. These effects are only in the presence of superfluid friction; when $\alpha \to 0$, we have $\sigma \to \eta$, and the normal fluid influence is nil.

In the small temperature limit (under 1 K), the normal fluid effects are negligible, as stated previously. It has been shown experimentally that the vortex lines are able to decay under these conditions.[29] It was assumed that occasional vortex reconnection gives rise to kinks on the vortex line. These kinks were considered as superpositions of Kelvin waves. Kelvin waves can lose energy by emitting sound (phonons), hence, the observed decay even in the absence of friction effects due to the normal fluid. For future work, it may be interesting to study the dynamics of Kelvin waves related to such filament kinks. In principle, these might best be modeled as the superposition of solitons on the filament (with the solitons representing decaying Kelvin waves), which makes sense in light of the fact that the standard LIA is integrable. This also has possible topological implications for the propagation of Kelvin waves along vortex filaments which demonstrate breakdown and reconnection. In particular, such solutions would break the similarity observed here. However, such similarity breaking would be of a distinct kind from that observed when U becomes non-negligible (as considered in Subsection V D). In such a case, the addition of a drift term is not likely to be sufficient, and a more involved approach to representing such solutions would be required.

ACKNOWLEDGMENTS

R.A.V. is supported in part by National Science Foundation (NSF) Grant No. 1144246.

[1] H. E. Hall and W. F. Vinen, "The rotation of liquid helium II. I. Experiments on the propagation of second sound in uniformly rotating helium II," Proc. R. Soc. London, Ser. A **238**, 204 (1956).
[2] H. E. Hall and W. F. Vinen, "The rotation of liquid helium II. II. The theory of mutual friction in uniformly rotating helium II," Proc. R. Soc. London, Ser. A **238**, 215 (1956).
[3] I. L. Bekarevich and I. M. Khalatnikov, "Phenomenological derivation of the equations of vortex motion in He II," Sov. Phys. JETP **13**, 643–646 (1961).
[4] L. D. Landau and E. M. Lifshitz, *Fluid Mechanics* (Addison and Wesley, 1959).
[5] K. W. Schwarz, "Three-dimensional vortex dynamics in superfluid ^{4}He: Line-line and line-boundary interactions," Phys. Rev. B **31**, 5782 (1985).

[6] L. S. Da Rios, "Sul moto d'un liquido indefinite con un filetto vorticoso di forma qualunque," Rend. Circ. Mat. Palermo **22**, 117 (1906).
[7] R. J. Arms and F. R. Hama, "Localized-induction concept on a curved vortex and motion of an elliptic vortex ring," Phys. Fluids **8**, 553 (1965).
[8] R. L. Ricca, "Rediscovery of Da Rios equations," Nature (London) **352**, 561 (1991).
[9] T. Lipniacki, "Shape-preserving solutions for quantum vortex motion under localized induction approximation," Phys. Fluids **15**, 1381 (2003).
[10] T. Lipniacki, "Quasi-static solutions for quantum vortex motion under the localized induction approximation," J. Fluid Mech. **477**, 321 (2003).
[11] S. Gutiérrez, J. Rivas, and L. Vega, "Formation of singularities and self-similar vortex motion under the localized induction approximation," Commun. Partial Differ. Equ. **28**, 927 (2003).
[12] B. Svistunov, "Superfluid turbulence in the low-temperature limit," Phys. Rev. B **52**, 3647 (1995).
[13] B. K. Shivamoggi, "Vortex motion in superfluid ^{4}He: Reformulation in the extrinsic vortex-filament coordinate space," Phys. Rev. B **84**, 012506 (2011).
[14] H. Hasimoto, "Motion of a vortex filament and its relation to elastica," J. Phys. Soc. Jpn. **31**, 293 (1971).
[15] H. Hasimoto, "A soliton on a vortex filament," J. Fluid Mech. **51**, 477 (1972).
[16] S. Kida, "A vortex filament moving without change of form," J. Fluid Mech. **112**, 397 (1981).
[17] R. A. Van Gorder, "Fully nonlinear local induction equation describing the motion of a vortex filament in superfluid ^{4}He," J. Fluid Mech. **707**, 585 (2012).
[18] R. A. Van Gorder, "Motion of a vortex filament in the local induction approximation: A perturbative approach," Theor. Comput. Fluid Dyn. **26**, 161 (2012).
[19] R. A. Van Gorder, "Integrable stationary solution for the fully nonlinear local induction equation describing the motion of a vortex filament," Theor. Comput. Fluid Dyn. **26**, 591 (2012).
[20] R. A. Van Gorder, "Scaling laws and accurate small-amplitude stationary solution for the motion of a planar vortex filament in the Cartesian form of the local induction approximation," Phys. Rev. E **87**, 043203 (2013).
[21] T. Araki, M. Tsubota, and S. K. Nemirovskii, "Energy spectrum of superfluid turbulence with no normal-fluid component," Phys. Rev. Lett. **89**, 145301 (2002).
[22] S. Z. Alamri, A. J. Youd, and C. F. Barenghi, "Reconnection of superfluid vortex bundles," Phys. Rev. Lett. **101**, 215302 (2008).
[23] W. F. Vinen, "Decay of superfluid turbulence at a very low temperature: The radiation of sound from a Kelvin wave on a quantized vortex," Phys. Rev. B **64**, 134520 (2001).
[24] M. Umeki, "A locally induced homoclinic motion of a vortex filament," Theor. Comput. Fluid Dyn. **24**, 383 (2010).
[25] M. Umeki, "A real-space representation of a locally induced vortex filament," Theor. Appl. Mech. Jpn. **61**, 195 (2013).
[26] R. A. Van Gorder, "Exact solution for the self-induced motion of a vortex filament in the arc-length representation of the local induction approximation," Phys. Rev. E **86**, 057301 (2012).
[27] V. Banica and L. Vega, "On the stability of a singular vortex dynamics," Commun. Math. Phys. **286**, 593–627 (2009).
[28] M. Tsubota, T. Araki, and S. K. Nemirowskii, "Dynamics of vortex tangle without mutual friction in superfluid ^{4}He," Phys. Rev. B **62**, 11751 (2000).
[29] S. I. Davis, P. C. Hendry, and P. V. E. McClintock, "Decay of quantized vorticity in superfluid ^{4}He at mK temperatures," Physica B **280**, 43 (2000).